Cellular Physiology and Biochemistry

Cell Physiol Biochem 2013;31:166-178
DOI: 10.1159/000343358
Published online: February 01, 2013
Accepted: January 10, 2013

1421-9778/13/0311-0166$38.00/0

Original Paper

Connexins and M3 Muscarinic Receptors Contribute to Heterogeneous Ca^{2+} Signaling in Mouse Aortic Endothelium

François-Xavier Boittin[a,c] Florian Alonso[b,c] Loïc Le Gal[b] Florent Allagnat[b] Jean-Louis Bény[a] Jacques-Antoine Haefliger[b]

[a]Department of Zoology and Animal Biology, Laboratory of Vascular Cell Physiology, University of Geneva, Geneva 4; [b]Service of Internal Medicine, Laboratory of Experimental Medicine, Department of Physiology, Lausanne; [c]These authors contributed equally to this work

Key Words
Gap junction • Connexin • Endothelium • Aorta • Calcium

Abstract
Background/Aims: Smooth muscle tone is controlled by Ca^{2+} signaling in the endothelial layer. Mouse endothelial cells are interconnected by gap junctions made of Connexin40 (Cx40) and Cx37, which allow the exchange of signaling molecules to coordinate their activity. Here, we investigated the role of Cx40 in the endothelial Ca^{2+} signaling of the mouse aorta. ***Methods:*** Ca^{2+} imaging was performed on intact aortic endothelium from both wild type (Cx40+/+) and Connexin40-deficient (Cx40-/-) mice. ***Results:*** Acetylcholine (ACh) induced early fast and high amplitude Ca^{2+} transients in a fraction of endothelial cells expressing the M3 muscarinic receptors. Inhibition of intercellular communication using carbenoxolone or octanol fully blocked the propagation of ACh-induced Ca^{2+} transients toward adjacent cells in WT and Cx40-/- mice. As compared to WT, Cx40-/- mice displayed a reduced propagation of ACh-induced Ca^{2+} waves, indicating that Cx40 contributes to the spreading of Ca^{2+} signals. The propagation of those Ca^{2+} responses was not blocked by suramin, a blocker of purinergic ATP receptors, indicating that there is no paracrine effect of ATP release on the Ca^{2+} waves. ***Conclusions:*** Altogether our data show that Cx40 and Cx37 contribute to the propagation and amplification of the Ca^{2+} signaling triggered by ACh in endothelial cells expressing the M3 muscarinic receptors.

Introduction

Ca^{2+} signaling in the endothelium is fundamental for the regulation of vascular tone and arterial blood pressure. There is a tight link between the spreading of Ca^{2+} waves occurring during agonist stimulation of endothelial cells and the subsequent relaxation of smooth

Dr. Jacques-Antoine Haefliger
Service of Internal Medicine, Laboratory of Experimental Medicine
Department of Physiology, Bugnon 7a, 1005 Lausanne (Switzerland)
Tel. +41 79 556 85 96, E-Mail Jacques-Antoine.Haefliger@chuv.ch

muscle cells. Indeed, agonists such as acetylcholine (ACh) trigger cytosolic Ca^{2+} increases in the endothelium which can mediate the production of vasodilators such as NO, PGI2 and the EDHF, depending on the vascular bed [1-3].

The endothelium of blood vessels is composed of endothelial cells which are interconnected by gap junction channels [4]. These channels are made of two connexons (also called hemichannels) whose association at intercellular junctions forms a functional pore enabling the diffusion of ions or intracellular messengers between adjacent cells [5]. In cultured endothelial cells, gap junctions allow the propagation of Ca^{2+} waves in the endothelial layer through the diffusion of Ca^{2+} or second messenger such as $InsP_3$ [6]. However, ATP release through hemichannels may also contribute to the propagation of Ca^{2+} waves by activating purinergic receptors on adjacent endothelial cells, in particular upon mechanical stimulation of endothelial cells [7, 8].

The mouse aortic endothelium express Connexin40 (Cx40) and Cx37 [9] and both isoforms are involved in the formation of functional gap junctions and diffusion of dyes between native endothelial cells [10, 11]. Cx40 may also form hemichannels releasing ATP among other molecules. In cultured renal glomerular endothelial cells, it has been hypothetized that the propagation of Ca^{2+} waves upon mechanical stimulation occurs through purinergic stimulation of adjacent cells [8].

Several studies described that the lack of Cx40 reduces the conducted vasodilation in different resistance vessels [12-14]. In addition, endothelial gap junctions have been shown to modulate vasomotor tone by regulating the release of relaxing factors such as NO and EDHF [12, 15-17]. Finally, Cx40 appears to be of major importance for the conduction of agonists-induced endothelium-dependent vasodilations along arterioles as it cannot be replaced by Cx45 [14].

In the intact mouse aortic endothelium, Ca^{2+} signaling upon agonist stimulation is either homogeneous in the case of ATP or highly heterogeneous in the case of ACh or other agonists [18]. However, the reasons for these differences have not been investigated so far. Here, we used Ca^{2+} imaging of intact aortic endothelium from wild type (Cx40+/+) and Cx40-deficient (Cx40-/-) mice to investigate the origin of heterogeneous Ca^{2+} signaling as well as the effect of Cx40 deficiency. We first show that while ATP triggered homogeneous Ca^{2+} signals in the endothelial layer, ACh triggers early fast and high amplitude Ca^{2+} increases in only a fraction of native endothelial cells. This heterogeneous response of the endothelium to global ACh stimulation is linked to the restricted expression of M3 muscarinic ACh receptors (M3-mAChRs) on a subpopulation of native endothelial cells. We then demonstrate that those early fast Ca^{2+} increases occurring in a limited fraction of native endothelial cells spread toward adjacent cells through endothelial gap junction channels, without the involvement of hemichannel-dependent ATP release. Altogether our results indicate that the heterogeneous cholinergic Ca^{2+} signaling of the mouse aortic endothelium is linked to both restricted M3-mAChRs expression and spreading of Ca^{2+} signals through gap junctions made of Cx40 and Cx37.

Materials and Methods

Animals

The investigation conforms to the Guide for the Care and Use of Laboratory Animals published by the US National Institutes of Health (NIH Publication, 8th Edition, 2011). Mouse care and euthanasia procedures were approved by our institution and the Veterinary Office (Lausanne, Switzerland), and conform to the guide for the care and use of laboratory animals (University of Lausanne, A555213-01). Cx40-deficient mice (Cx40-/- deleted for the gap junction alpha-5 protein) were a gift from Dr. K. Willecke [19]. Breeding pairs of Cx40-/- mice were crossed with control C57/Bl6 partners. Homozygous Cx40-/- and wild type mice (Cx40+/+) were then identified using PCR of genomic DNA. Primers used for PCR were as follow: for the Cx40 recombinant allele (494 bp), 5'-GGATCGGCCATTGAACAAGATGGATTGCAC-3'

(sense) and 5'-CTGATGCTCTTCGTCCAGATCATCCTGATCG-3' (antisense); for the Cx40 wild type allele (314 bp), 5'-GGGAGATGAGCAGGCCGACTTCCGGTGCG-3' (sense) and 5'-GTAGGGTGCCCTGGAGGACAATCTTCCC-3' (antisense). Mice used in the experiments were from litters obtained after at least 10 backcrosses into the C57/Bl6 background. Males of three- to five-month-old Cx40 knock-out (Cx40-/-) and wild type controls (Cx40+/+) were used for all experiments.

Ca^{2+} measurements in the endothelial layer of fresh mouse aortic strips

Anesthetized Cx40-/- and Cx40+/+ mice with 2-bromo-2-chloro-1,1,1-trifluoroethane, were killed by cervical dislocation and the thoracic aorta was quickly removed, cleaned and opened longitudinally. Aortic strips (of around 1 mm^2) were then cut for Ca^{2+} measurements or immunostaining of native aortic endothelial cells. Ca^{2+} measurements in the endothelial layer of mouse aortic strips were performed as previously described [20]. Briefly, aortic strips were loaded for 1 h at 37°C with Fluo-4AM (50 µM) in a solution containing (in mM): 140 NaCl, 5.6 KCl, 1 $MgCl_2$, 2 $CaCl_2$, 10 Glucose and 10 Hepes, pH 7.4. After being loaded, aortic strips were washed and clamped horizontally in the experimental chamber with the endothelial layer above. Dye-loaded aortic strips were then used for Ca^{2+} imaging experiments, using an Olympus upright microscope equipped with a 40× water immersion extra-long working distance objective. Aortic strips were excited between 460 and 490 nm and the emitted fluorescence from Fluo-4AM-loaded endothelial cells was collected between 515 and 550 nm using a Photometric Cool Snap camera. Before each experiment, the cellular integrity of the tissue was assessed by capturing Fluo-4 fluorescence images to visualize the endothelial nuclei as demonstrated in Figure 1A. Image acquisition and data analysis were performed using IPLab software (Scanalytics, Inc). Images of the endothelial monolayer were acquired at a 2 Hz frequency in all experiments. For analysis, self-ratio (Fluo-4 ratio) were calculated by dividing all images from time series by the first one (Fluo-4 ratio=Fluorescence/Fluorescence at rest). Hence, no change in Fluo-4 fluorescence corresponds to Fluo-4 ratio=1. Fluo-4 ratio traces represent measurements performed in single endothelial cells. All measurements were performed using IPLab and Excel software. As previously mentioned, significant contamination of endothelial cells Fluo-4 fluorescence by fluorescence arising from the smooth muscle layer can be excluded [20]. Moreover, we have previously reported that ACh does not trigger contraction of the smooth muscle layer in the mouse aorta [21]. In Figures 2C and 6C, the "% of whole field surface" represents the percentage of the whole field surface (76800 μm^2) that shows Ca^{2+} increases (>1.02 in Fluo-4 ratio) in response to bath application of ACh in control conditions or after preincubation of aortic strips with carbenoxolone, 1-octanol or suramin. For experiments shown in Figures 2A and 6B, a control ACh stimulation of the same field of endothelial cells was performed prior to preincubation with carbenoxolone and further ACh stimulation.

Western blotting

Aortas were excised, rapidly placed into liquid nitrogen, reduced to powder, and homogenized by sonication in SDS Lysis Buffer (62.5 mM Tris-EDTA, pH 6.8, 5% SDS). Samples were processed as published [9, 15]. To prepare enriched endothelial cells samples, aortas were longitudinally opened in 100 µl PBS, and pinned on silicone, endothelium-side up. A scalpel was used to gently scrape off endothelial cells. Aliquots of endothelial cells were homogenized in SDS Lysis Buffer. Samples were equally loaded on a 10% polyacrylamide gel followed by electrophoresis and transferred onto PVDF membrane (Immobilon-P; Millipore, Volketswil, Switzerland). Protein content was measured using a detergent-compatible DC protein assay kit (Bio-Rad Laboratories, Reinach BL, Switzerland). Membranes were incubated for 1 hour in PBS containing 5% milk and 0.1% Tween20 (blocking buffer). Saturated membranes were incubated overnight at 4°C with rabbit anti-muscarinic ACh Receptor M3 (H-210) antibody (Sc-9108, 1/500, Santa Cruz Biotechnology, Inc), rabbit anti-Cx40 antibody (AB1726; 1:250, Chemicon), rabbit anti-Cx37 antibody (Cx37A11-A, 1:1000, Biotrend Chemikalien GmbH) or monoclonal antibody anti-alpha-tubulin (T5168, Sigma-Aldrich, 1:3000). After incubation at room temperature for 1 hour with a convenient secondary antibody conjugated to horseradish peroxidase (Fluka Chemie, diluted 1:20,000), membranes were revealed by enhanced chemiluminescence (ECL) according to the manufacturer's instructions (Amersham Bioscience Europe). Densitometric analyses of immunolabeled proteins (western blots) were performed using the ImageQuant Software (Molecular Dynamics, Amersham BioscienceEurope).

En face immunostaining of muscarinic ACh receptors M3 and endothelial Connexins

Aortic strips from mouse thoracic aorta were clamped horizontally with the endothelial layer above in siliconed Petri dishes containing PBS. Aortic strips were fixed with 100% ethanol for 15 min at -20°C, washed and incubated with PBS containing 0.1% Triton X100 and 0.5% BSA for 15 min. After saturation, aortic strips were incubated overnight with a rabbit anti-(M3-mAChRs) (H-210) antibody (Sc-9108, 1/50, Santa Cruz Biotechnology, Inc) in PBS containing 0.1% Triton X100 and 0.5% BSA [22, 23]. After extensive washing, aortic strips were incubated for 1 h with an Alexa Fluor 488-conjugated donkey anti-rabbit antibody (Invitrogen) in PBS containing 0.1% Triton X100 and 0.5% BSA. Aortic strips were then washed and mounted in PBS containing 50% glycerol and 0.4µg/mL of DAPI before observation of the endothelial layer with a fluorescence microscope (Leica Leitz DMRB, Nidau, Switzerland). Control experiments were performed by omitting the primary antibody. The % of endothelial cells stained with the M3-mAChRs antibody was assessed using ImageJ software. For M3 receptor/Cx40 and M3 receptor/Cx37 double immunostainings in aortic endothelium (Fig. 4), a goat polyclonal antibody specific to mouse M3-mAChRs was used (Sc-7474, 1/50, Santa Cruz Biotechnology, Inc) and incubated simultaneously with rabbit polyclonal antibody specific to either mouse Cx40 (AB1726, 1/50, Millipore) or mouse Cx37 (Cx37A11-A, 1/50, Biotrend Chemikalien GmbH). Primary antibodies were detected using donkey anti-goat immunoglobulins labeled with Alexa Fluor 488 and donkey anti-rabbit immunoglobulins labeled with Alexa Fluor 594 (Invitrogen). For Cx40/Cx37 double immunostaining in aortic endothelium (Fig. 5), a mouse monoclonal antibody specific to mouse Cx40 was used (37-8900, Invitrogen, 1/200) and was detected using anti-mouse immunoglobulins labeled with Alexa Fluor 594 (Invitrogen).

Chemicals

Acetylcholine (ACh), Adenosine 5'-triphosphate (ATP), carbenoxolone (3β-Hydroxy-11-oxoolean-12-en-30-oic acid 3-hemisuccinate) and suramin were from Sigma. Fluo-4AM was purchased from Molecular probes.

Statistical analysis

Results are expressed as mean ± SEM. The number of mice used is indicated in the figure legends. One-way ANOVA was performed to compare the mean values between groups, using the post hoc Bonferroni test, as provided by The Statistical Package for the Social Science (SPSS 17.0, Chicago, IL). Student's *t*-test was used to compare data from two groups. *P* values of <0.05 were considered as significant.

Results

Heterogeneity of ACh-induced Ca^{2+} responses in the intact mouse aortic endothelium

Ca^{2+} imaging of intact aortic endothelium from Cx40+/+ and Cx40-/- mice was used to investigate the origin of heterogeneous Ca^{2+} signaling in response to global ACh stimulation. Global stimulation of the intact endothelium (Fig. 1A) of Cx40+/+ aortic strips with 10 µM ACh triggered Ca^{2+} increases in only a fraction of native endothelial cells (Fig. 1B), whereas ATP stimulated Ca^{2+} increases in all endothelial cells of the field (Fig. 1C). Examination of ACh-induced Ca^{2+} increases in individual endothelial cells revealed highly heterogeneous Ca^{2+} responses in term of amplitude and kinetic among the population of endothelial cells displaying Ca^{2+} increases (Fig. 1D). Some endothelial cells responded by an early fast and high amplitude biphasic Ca^{2+} increase composed by a peak and a plateau phase (see picture 5 and representative Ca^{2+} responses (cell a or d) in Fig. 1B and D), and are surrounded by cells displaying slower Ca^{2+} increases of lower amplitude (see picture 6 and Ca^{2+} responses for cells b and c or e and f in Fig. 1B and D) whose amplitude attenuates with the distance from cell a or d. This suggests that the fast biphasic Ca^{2+} increases occurring in some endothelial cells (for example cell a or d) spread towards adjacent cells (cells b and c or e and f, Fig. 1B and D). In contrast, ATP induced a fast and high amplitude Ca^{2+} increases (also composed by a peak and a plateau phase) that were synchronous and of similar amplitude and kinetic in all endothelial cells of the same field (cells a, b, c, d, e and f; Fig. 1C and D).

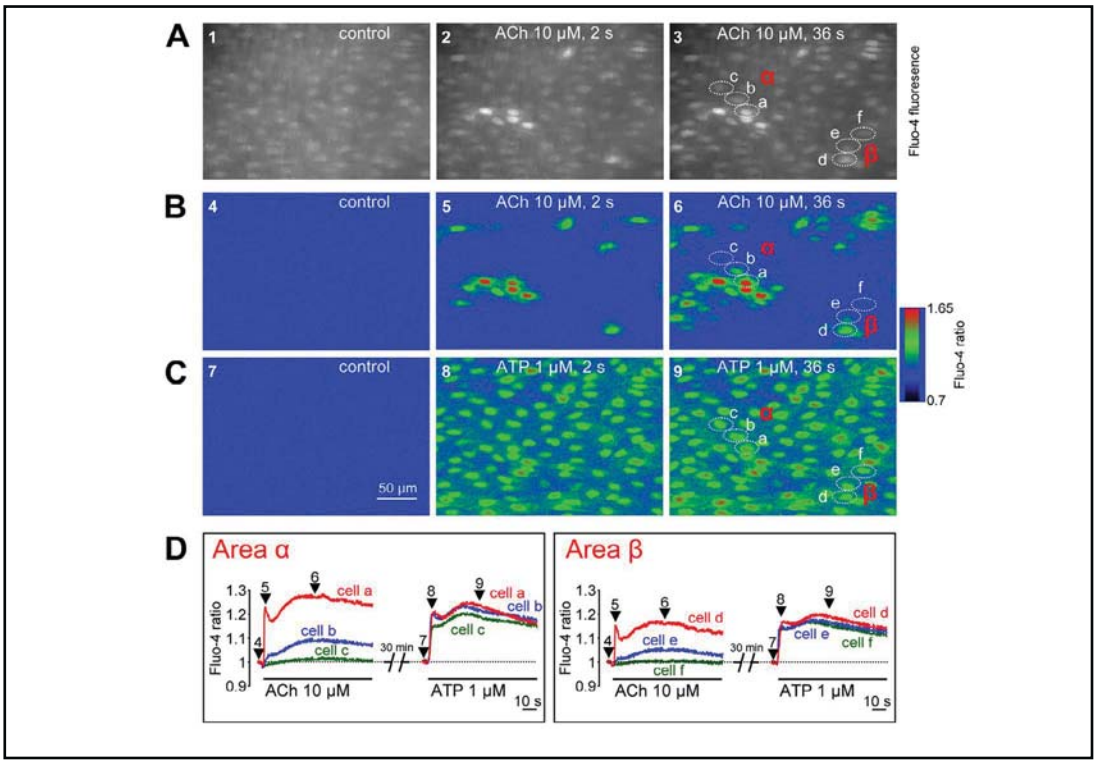

Fig. 1. Heterogeneity of ACh-induced Ca^{2+} responses in the intact aortic endothelium from Cx40+/+ mice. A: Time sequences of the Fluo-4 fluorescence images (in black and white to see the fluorescence background in all the endothelium) from left to right before (image 1: control) and 2 seconds (s) and 36 s (image 2 and 3 respectively) after global ACh (10 µM) stimulation of the endothelium. Fluo-4 fluorescence shows that endothelium is intact as demonstrated by the visualization of the endothelial nuclei. B: Images 4, 5 and 6 represent time sequences of Fluo-4 ratio images (corresponding to the experiment shown in panel A) before (image 4: control) and 2 and 36 s (images 5 and 6 respectively) after global ACh (10 µM) stimulation of the endothelial cells field a showing the evolution of Fluo-4 ratio in the endothelium after global ACh stimulation. C: images 7, 8 and 9 represent time sequences of Fluo-4 ratio images before (image 7: control) and 2 and 36 s (images 8 and 9 respectively) after global ATP (1 µM) stimulation of the same endothelium field shown in panels A and B. D: Time course of the Fluo-4 ratio in individual endothelial cells (cells a, b, c, d, e, and f, indicated by dotted ovals on images 3, 6 and 9) from two different areas of the endothelium (areas α and β). For each individual endothelial cell, the time course of ACh- and ATP-induced Ca^{2+} increases is represented. Arrows on the graphs indicate the time corresponding to the pictures shown in panels B and C. Stimulation of the endothelium with ATP was performed 30 min after ACh stimulation and after extensive washing of ACh to allow recovery to basal Ca^{2+} levels in the endothelium. This experiment is representative from 5 independent trials.

ACh-induced Ca^{2+} responses involve interendothelial cells communication in the mouse aortic endothelium

To investigate whether the spreading of ACh-induced Ca^{2+} increases occurs through gap junction channels or through a paracrine effect of ATP, we tested the effect of gap junction and purinergic receptor inhibition on the ACh-induced Ca^{2+} responses of Cx40+/+ aortic strips [24, 25]. As shown in Fig. 2A, preincubation of Cx40+/+ aortic strips with the gap junction inhibitor carbenoxolone (100 µM) completely inhibited the spreading of the fast biphasic Ca^{2+} increase occurring in cell (a) toward adjacent cells (b or c) while the amplitude of the fast ACh-induced Ca^{2+} increase of cell (a) remained unaffected (Fig. 2A-B). On the contrary, preincubation of Cx40+/+ aortic strips with the purinergic antagonist suramin (200µM), did not inhibit the spreading of ACh-induced fast Ca^{2+} increases (Fig. 2B). As a positive control,

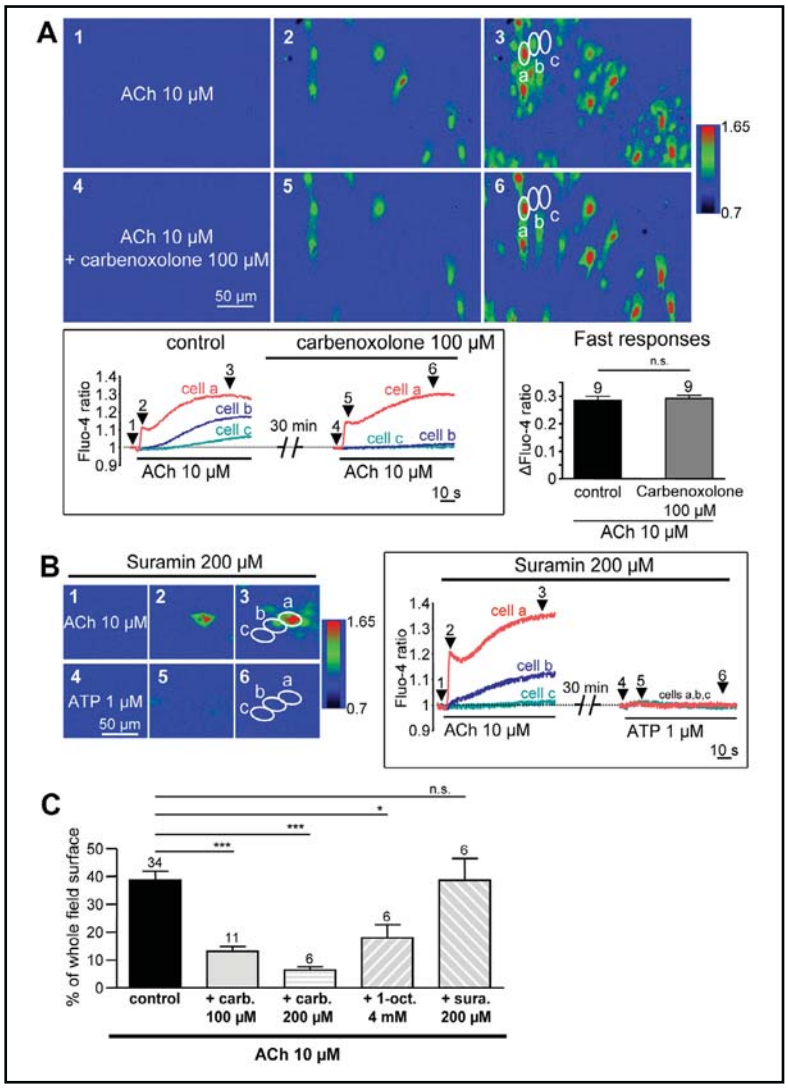

Fig. 2. Gap junction blockers decrease the ACh-induced Ca^{2+} responses in the endothelium from Cx40+/+ mice. A: Effect of carbenoxolone (100 µM) on ACh-induced Ca^{2+} increases in the endothelium from Cx40+/+ mice. The image panel represent time sequences of Fluo-4 ratio images before (images 1 and 4) and after global ACh stimulation of the same Cx40+/+ aortic strip in absence (images 1, 2 and 3) or in presence of carbenoxolone (100 µM, images 4, 5 and 6). After the first ACh response, the aortic strip was washed and pretreated for 30 min with carbenoxolone prior to ACh application. The lower panel (left) shows the time course of Fluo-4 ratio in individual endothelial cells (cells a, b and c, indicated on images by ovals) in control and after a 30 min preincubation with carbenoxolone (100 µM). Arrows on the graphs indicate the time corresponding to the pictures shown. The bar chart on the right represents the average amplitude of ACh-induced Ca^{2+} increases in 9 cells displaying fast biphasic Ca^{2+} increases in control and after preincubation with 100 µM carbenoxolone (n.s.: not significant). This experiment is representative from 6 independent trials. B: Effect of suramin (200 µM) on ACh- and ATP-induced Ca^{2+} increases in the endothelium from Cx40+/+ mice. The left panel shows time sequences of Fluo-4 ratio images corresponding to the evolution of Fluo-4 ratio after ACh and ATP (1 µM) stimulation of the same aortic strip in the presence of suramin (200 µM). The right panel shows the time course of Fluo-4 ratio in individual endothelial cells (cells a, b and c, indicated on the third picture of the left pannel) for ACh and ATP stimulation. C: Average values showing the effect of carbenoxolone (carb. 100 and 200 µM), 1-octanol (1-oct. 4 mM) and suramin (sura. 200 µM), preincubated 30 min on the % of whole field surface responding to ACh by Ca^{2+} increases in the aortic endothelium from Cx40+/+ mice. Numbers of experiments performed from 14 Cx40+/+ mice are indicated above bars.

we observed that suramin fully blocked the Ca^{2+} responses to exogenous ATP (Fig. 2B). Quantitative assessment of the percentage of cells showing Ca^{2+} responses confirmed that suramin had no impact of the Ca^{2+} wave propagation while carbenoxolone, at 100 or 200 µM, fully blocked the spreading. Similar results were obtained when Cx40+/+ aortic strips were pre-incubated with 1-Octanol (4 mM), another gap junction inhibitor (Fig. 2C).

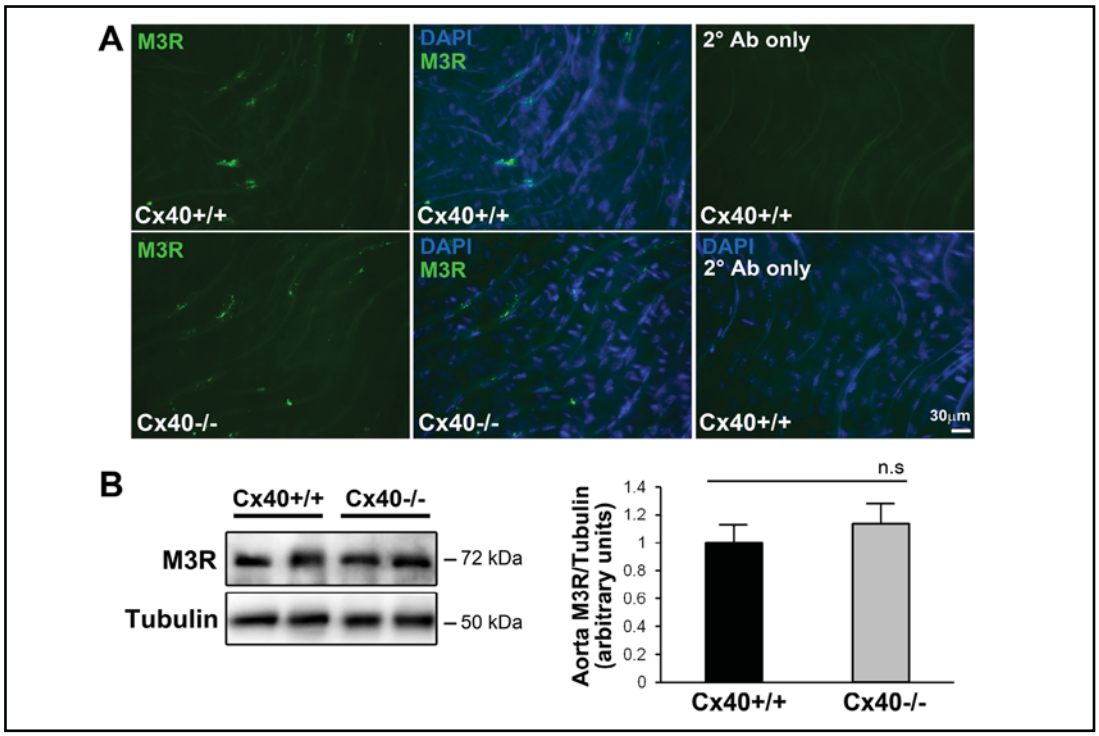

Fig. 3. Immunolocalization and expression levels of M3 muscarinic ACh receptors in the aortic endothelium. A: En-face staining of M3 muscarinic ACh receptors in intact endothelium from Cx40+/+ and Cx40-/- mice (representative from 3 independent experiments). Left panel: immunostaining for M3 muscarinic ACh receptors (M3R) in intact endothelium from aortas of Cx40+/+ (upper) and Cx40-/- (lower) mice. Middle panel: immunostaining for M3 muscarinic ACh receptor (M3R) counterstained with DAPI to visualize nuclei of endothelial cells. Right panel: negative control by omitting the anti-M3 muscarinic ACh receptor (M3R) antibody in Cx40+/+ mice. B: Left panel: A representative Western blot of whole aortas from Cx40-/- and Cx40+/+ mice showing the expression levels of the M3 muscarinic ACh (M3R) receptor as well as Tubulin. Right: Quantitative assessment of the immunolabeled bands corresponding to the muscarinic ACh receptor (M3R) proteins normalized to Tubulin in the aorta from Cx40-/- and Cx40+/+ mice (6 Cx40+/+ and 6 Cx40-/- mice) (n.s.: not significant).

Immunolocalization of M3 muscarinic ACh receptors in the mouse aortic endothelium

The endothelium from Cx40+/+ and Cx40-/- mouse aortic strips was immunostained using an anti-M3 muscarinic ACh receptors (M3-mAChRs) antibody [22, 23]. M3-mAChRs staining was detected in only a fraction of endothelial cells both in Cx40+/+ and Cx40-/- mice (Fig. 3A). In Cx40+/+ mice, analysis revealed that M3-mAChRs were present in only 5.9 ± 0.5% (n=3) of endothelial cells (data not shown). Therefore, the heterogeneous pattern of ACh responses observed in the mouse aortic endothelium could be linked to the heterogeneous expression of M3-mAChRs. In addition, Western Blot analysis of whole aorta of Cx40-/- and Cx40+/+ mice revealed that M3-mAChRs expression levels were not significantly different in the Cx40-/- mice when compared to control mice (Cx40+/+) (Fig. 3B).

Expression of the M3 muscarinic ACh receptors and the Cx40 and Cx37 in the aortic endothelium

To evaluate whether the fraction of endothelial cells expressing M3-mAChRs expresses gap junctions made of Cx40 and Cx37, we performed double immunostaining on "en face" aortic endothelium. Combining Cx40 (in red) with M3-mAChRs (in green) antibodies revealed the presence of Cx40 at regions of cell-cell contact between endothelial cells expressing M3-

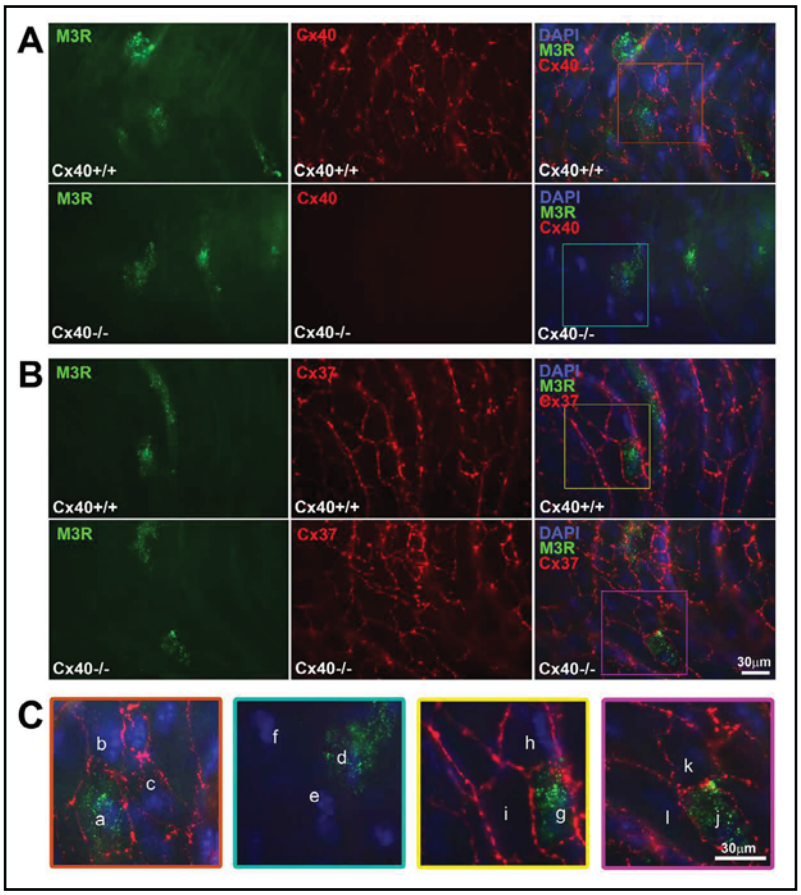

Fig. 4. Immunolocalization of the M3 muscarinic ACh receptors and the Cx40 and Cx37 in the aortic endothelium. A: En face double immunolabeling of aortic endothelium of Cx40+/+ and Cx40-/- mice for muscarinic ACh receptor (M3R, green) and Cx40 (red). M3R staining was found limited to a fraction of endothelial cells and revealed a distribution of the receptor over the entire luminal surface of the cells. Cx40 staining clearly outlined the regions of cell-cell contact of each endothelial cell by discontinuous beaded strands of fluorescence label. Cx40 was absent in the Cx40-/- mice whereas muscarinic ACh receptor was not altered. B: En face double immunolabeling of aortic endothelium of Cx40+/+ and Cx40-/- mice for muscarinic ACh receptor (green) and Cx37 (red). In Cx40-/- mice endothelial cells expressing the muscarinic ACh receptor are connected to each other by Cx37 as observed by the presence of a punctuate staining around the endothelial cells. C: Higher magnification of the boxed area shown in A and B in the merged pictures show a M3R and Cx40 expressing endothelial cell (cells a, d, g and j) and the adjacent endothelial cells expressing only Cx40 and/or Cx37-/- (cells b, c, e, f, h, i, k and l). This experiment revealed that in Cx40-/- mice, endothelial cells expressing the muscarinic ACh receptor are only coupled to surrounding endothelial cells through Cx37. Data are representative from 3 independent experiments. DAPI staining was used to visualize nuclei of endothelial cells.

mAChRs and adjacent endothelial cells in Cx40+/+ mice (Fig. 4A, upper panels). Consistently, Cx40 was not detected in the aortic endothelium of Cx40-/- mice (Fig. 4A, lower panels). Immunofluorescence studies using Cx37 (in red) and M3-mAChRs antibodies revealed that endothelial cells expressing M3-mAChRs also express Cx37 at plasma membrane both in Cx40+/+ and Cx40-/- mice (Fig. 4B and C). The expression of Cx37 was similar in the endothelial cells expressing the M3 muscarinic receptor compared to the surrounding endothelial cells. These data demonstrate that, in Cx40+/+ mice, the fraction of endothelial cells expressing M3-mAChRs formed gap junctions made of Cx40 and Cx37 with neighboring cells whereas in Cx40-/- mice, this subpopulation of endothelial cells can only communicate with adjacent cells through channels made of Cx37. Double immunolabeling of Cx40 and Cx37 of "en face" preparations showed a colocalization of Cx40 and Cx37 at the membrane of endothelial cells in Cx40+/+ mice. No Cx40 was detected in the endothelium of Cx40-/- mice and the Cx37 immunolabeling was decreased in those mice (Fig. 5A). Immunoblots analysis of an enriched fraction of freshly scraped endothelial cells of aortas revealed a 50% decrease in Cx37 levels in the aortic endothelium of Cx40-/- mice compared to Cx40+/+ animals (Fig. 5B). Cx43 [9] or Cx32 [26] were not expressed in endothelial cells of Cx40+/+ or Cx40-/- mice (data not shown).

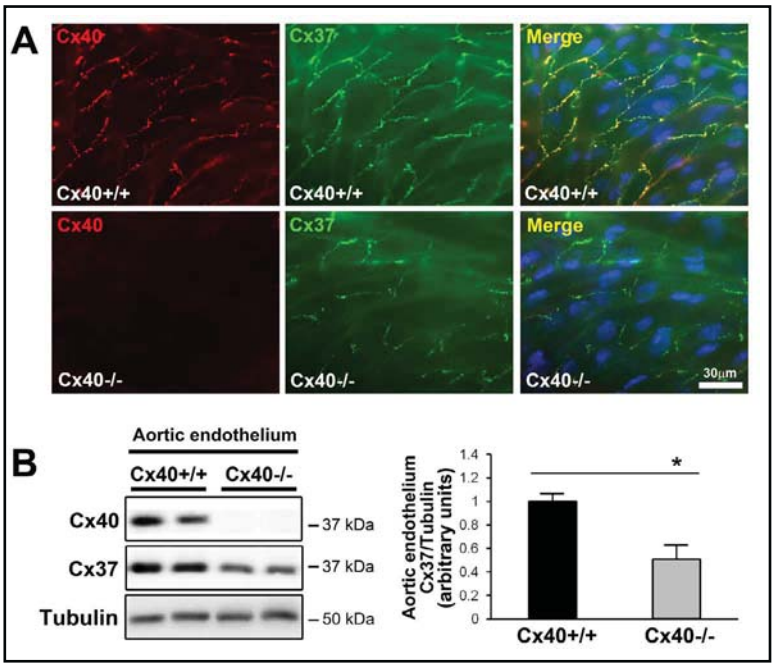

Fig. 5. Decreased Cx37 expression in the aortic endothelium of Cx40-/- mice. A: Antibodies detected Cx40 and Cx37 between aortic ECs of Cx40+/+ mice whereas no Cx40 and decreased Cx37 levels were found in ECs of Cx40-/- mice. B: Western blot analysis performed on enriched aortic endothelial cells samples confirmed the absence of Cx40 and revealed a 50 % decrease of Cx37 levels in the endothelium of Cx40-/- mice. (8 Cx40+/+ and 8 Cx40-/- mice).

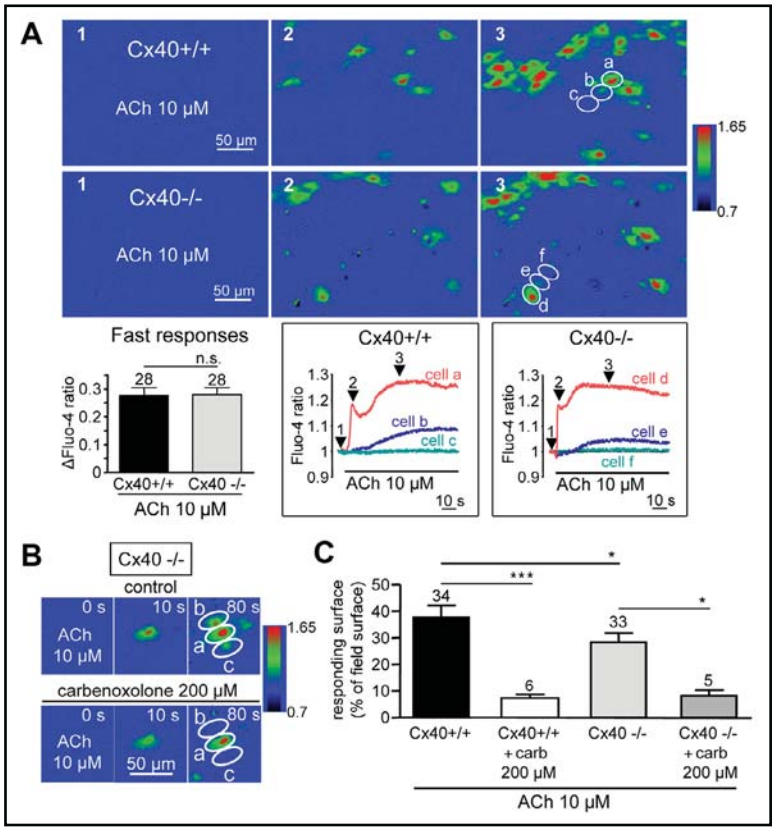

Fig. 6. Altered ACh-induced Ca^{2+} responses in the endothelium from Cx40-/- mice. A: Time sequences of Fluo-4 ratio images corresponding to the evolution of Fluo-4 ratio in endothelial cells after ACh stimulation of aortic strips from Cx40+/+ and Cx40-/- mice. The bar chart on the left represents the average amplitude of fast biphasic ACh-induced Ca^{2+} increases in endothelial cells from Cx40+/+ and Cx40-/- mice (n.s.: not significant). The lower panels (right) are representative time course of the Fluo-4 ratio in individual endothelial cells indicated on the upper image (a, b and c for Cx40+/+; d, e and f for Cx40-/-). B: Time sequences of Fluo-4 ratio images in endothelial cells after ACh stimulation of the same Cx40-/- aortic strip in control and after preincubation with carbenoxolone (200 µM) for 30 min. This experiment is representative from five independent trials. C: Average values showing the % of whole field surface responding to ACh in the aortic endothelium from Cx40+/+ or Cx40-/- mice preincubated or not with carbenoxolone (200 µM, 30 min preincubation). The numbers above bars correspond to the total number of fields used for quantification. Data are mean ± SEM.

ACh-induced Ca^{2+} responses in the intact endothelium from wild type (Cx40+/+) and Cx40-/- mice

Intercellular dye transfer experiments indicate that gap junctions made of Cx40 and Cx37 participate in cell-cell communication between endothelial cells [10, 11]. To assess the contribution of Cx40 and Cx37 in the spreading of ACh-induced Ca^{2+} responses, we investigated ACh-induced Ca^{2+} responses in the aortic endothelium from Cx40-/- mice, featuring also reduced Cx37 levels in the aortic endothelium [11, 15]. As shown in Fig. 6A, the amplitude of the early fast biphasic Ca^{2+} increases was not different in Cx40-/- mice when compared to their wild type littermate, indicating that the transduction pathway activated upon ACh stimulation is not altered in the endothelium from these mice. The propagation of ACh-induced fast Ca^{2+} increases toward adjacent cells was still observed in Cx40-/- mice (Fig. 6A-B). However quantitative assessment of the responding area revealed that the spreading was significantly reduced by about 25% in Cx40-/- compared to Cx40+/+ mice (28 ± 4% (n = 33) and 38.6 ± 3.2% (n = 34) for Cx40-/- and Cx40+/+ mice respectively) (Fig. 6C). As a negative control of propagation, we observed that this spreading was completely blocked upon carbenoxolone treatment in Cx40+/+ and Cx40-/- mice, (Fig. 6B-C). Of note, carbenoxolone did not alter the amplitude of the fast biphasic Ca^{2+} increases (data not shown).

Discussion

We showed that ACh but not ATP stimulation evokes Ca^{2+} increases in a fraction of native endothelial cells from mouse aorta (~40%) as already observed [18]. In rat thoracic aorta, a similar heterogeneity was observed in endothelial cells in response to ACh [27]. Our finding that M3 muscarinic ACh receptors (M3-mAChRs) are expressed in a fraction of endothelial cells likely explain these results, as ACh-induced endothelial Ca^{2+} responses and relaxation have been demonstrated to rely on the activation of these receptors in the mouse aorta [21, 28]. On the contrary to those evoked by ATP, ACh-induced Ca^{2+} responses were found to be highly heterogeneous among native endothelial cells. While a fraction of cells displayed early fast and high amplitude biphasic Ca^{2+} increases, adjacent cells showed lower and slower increases in Ca^{2+}. Our results demonstrate that the Ach-induced early fast biphasic Ca^{2+} increases spread toward adjacent cells through gap junction channels, as attested by its blockade by the gap junction blockers carbenoxolone or 1-octanol. Such spreading of ACh-induced Ca^{2+} signals is in accordance with dye transfer experiments showing extensive coupling between endothelial cells from the mouse aorta [10, 11]. In line with the work of Berra-Romani et al. [29], our results show homogenous endothelial Ca^{2+} signaling in response to ATP stimulation. In contrast to these results, Kameritsch et al., recently reported heterogeneous Ca^{2+} responses to ATP and demonstrated a role for endothelial gap junctions in the spreading of Ca^{2+} signaling in response to ATP stimulation [30]. This discrepancy could be due to differences in ATP concentrations used to stimulate endothelial cells or in the portion of the aorta used to perform the experiments.

The blockade of purinergic receptors did not prevent the spreading of the fast ACh-induced Ca^{2+} increases, indicating that there was no paracrine effect of ATP released through hemichannels and/or pannexin channels. Therefore, in contrast to the response of mechanically stimulated cells, which involves an ATP-dependent paracrine effect [8], the propagation of ACh-induced Ca^{2+} increases is probably mediated by the intercellular diffusion of Ca^{2+}, $InsP_3$ or other intracellular messengers though gap junction channels [5, 6, 31-33].

Only ~6% of endothelial cells still displayed Ca^{2+} increases upon ACh stimulation when the propagation of the Ca^{2+} waves was completely blocked using the gap junction channel inhibitor carbenoxolone. Immunofluorescent experiments further revealed that about 6% of the cells express the M3-mAChRs. Although it was not possible to perform M3 muscarinic receptors staining on the same preparation used for Ca^{2+} imaging, our data thus strongly suggest that the cells responding to ACh are those expressing the M3-mAChRs. Our results

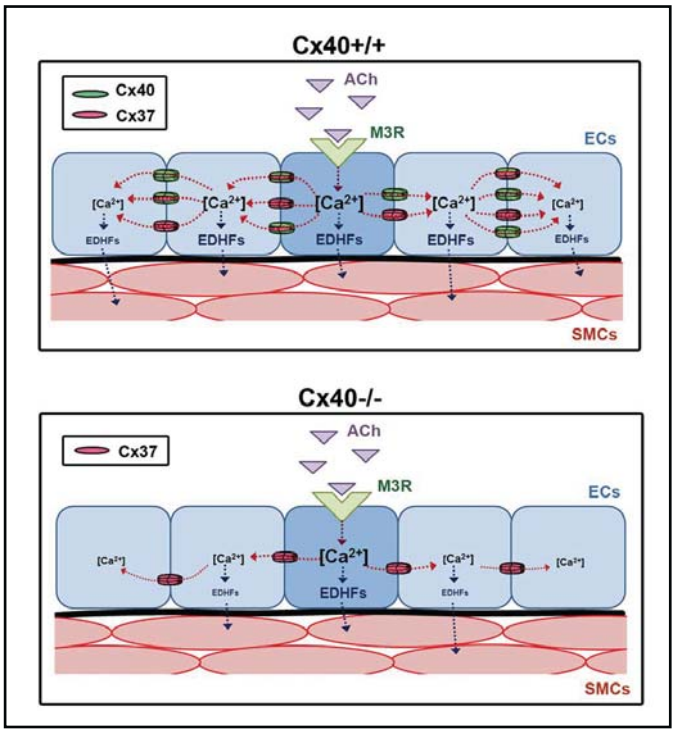

Fig. 7. Role of endothelial connexins in the ACh-induced Ca^{2+} signaling. In Cx40+/+ mice, during ACh stimulation, endothelial connexins mediates the spreading of Ca^{2+} signals from endothelial cells expressing the M3 muscarinic receptor to neighboring cells. In Cx40-/- mice, the absence of Cx40 and the decrease of Cx37 levels impact on the efficiency of the ACh-induced calcium signaling between endothelial cells.

also demonstrate that the percentage of cells exhibiting Ca^{2+} increases is reduced by 25% in Cx40-/- mice compared to Cx40+/+ mice. Interestingly, the percentage of ACh-responsive cells after gap junction blockade was similar in Cx40-/- and Cx40+/+ mice, indicating that the proportion of endothelial cells responding to ACh after gap junctions inhibition is not altered in Cx40-/- mice. Therefore, the reduced ACh-responding surface in Cx40-/- mice is mainly due to a reduction of the propagation of ACh-induced Ca^{2+} transients between endothelial cells, hence due to impaired gap junctional coupling. However the ACh-induced Ca^{2+} waves still occurred in the Cx40-/- aortic endothelium. Cx37 expression levels are reduced in the aortic endothelium from Cx40-/- mice and it was shown that both Cx40 and Cx37 participate to gap junction-dependent coupling in the mouse aortic endothelium [10, 11, 15]. Thus, the remaining Cx37 expression seems sufficient to build functional gap junctions allowing the spreading of Ca^{2+} responses in the Cx40-/- aortic endothelium [15]. Therefore our results suggest that both Cx40 and Cx37 are functional components of inter-endothelial cells gap junctions enabling the spreading of ACh-induced Ca^{2+} increases (Fig. 7). In conclusion, we show that the highly heterogeneous cholinergic Ca^{2+} signaling in the mouse aortic endothelium is due to restricted M3-mAChRs expression on a subpopulation of endothelial cells and propagation of Ca^{2+} signals through gap junction channels composed of Cx40 and Cx37.

Grants

This work was supported by grants from the Swiss National Science Foundation (3100A0-100098, 31003A-138528), the Donation Georges and Antoine Claraz, the Octav and Marcela Botnar Foundation and the Novartis and Muschamp Foundations.

Disclosures

No conflicts of interest are declared by the authors.

References

1 Tiruppathi C, Minshall RD, Paria BC, Vogel SM, Malik AB: Role of Ca^{2+} signaling in the regulation of endothelial permeability. Vascul Pharmacol 2002;39:173-185.
2 Freichel M, Suh SH, Pfeifer A, Schweig U, Trost C, Weissgerber P, Biel M, Philipp S, Freise D, Droogmans G, Hofmann F, Flockerzi V, Nilius B: Lack of an endothelial store-operated Ca^{2+} current impairs agonist-dependent vasorelaxation in TRP4-/- mice. Nat Cell Biol 2001;3:121-127.
3 de Wit C, Hoepfl B, Wolfle SE: Endothelial mediators and communication through vascular gap junctions. Biol Chem 2006;387:3-9.
4 Figueroa XF, Duling BR: Gap junctions in the control of vascular function. Antioxid Redox Signal 2009;11:251-266.
5 Harris AL: Connexin channel permeability to cytoplasmic molecules. Prog Biochem Biophys 2007;94:120-143.
6 Carter TD, Chen XY, Carlile G, Kalapothakis E, Ogden D, Evans WH: Porcine aortic endothelial gap junctions: Identification and permeation by caged InsP3. J Cell Sci 1996;109:1765-1773.
7 Gomes P, Srinivas SP, Vereecke J, Himpens B: ATP-dependent paracrine intercellular communication in cultured bovine corneal endothelial cells. Invest Ophth Vis Sci 2005;46:104-113.
8 Toma I, Bansal E, Meer EJ, Kang JJ, Vargas SL, Peti-Peterdi J: Connexin40 and ATP-dependent intercellular calcium wave in renal glomerular endothelial cells. Am J Physiol-Regul Integr Comp Physiol 2008;294:R1769-1776.
9 Alonso F, Krattinger N, Mazzolai L, Simon A, Waeber G, Meda P, Haefliger JA: An angiotensin II- and nf-kappab-dependent mechanism increases connexin43 in murine arteries targeted by renin-dependent hypertension. Cardiovasc Res 2010;87:166-176.
10 Kruger O, Beny JL, Chabaud F, Traub O, Theis M, Brix K, Kirchhoff S, Willecke K: Altered dye diffusion and upregulation of connexin37 in mouse aortic endothelium deficient in connexin40. J Vasc Res 2002;39:160-172.
11 Simon AM, McWhorter AR: Decreased intercellular dye-transfer and downregulation of non-ablated connexins in aortic endothelium deficient in connexin37 or connexin40. J Cell Sci 2003;116:2223-2236.
12 de Wit C, Roos F, Bolz SS, Kirchhoff S, Kruger O, Willecke K, Pohl U: Impaired conduction of vasodilation along arterioles in connexin40-deficient mice. Circ Res 2000;86:649-655.
13 Figueroa XF, Duling BR: Dissection of two cx37-independent conducted vasodilator mechanisms by deletion of cx40: Electrotonic versus regenerative conduction. Am J Physiol Heart Circul Physiol 2008;295:H2001-H2007.
14 Wolfle SE, Schmidt VJ, Hoepfl B, Gebert A, Alcolea S, Gros D, de Wit C: Connexin45 cannot replace the function of connexin40 in conducting endothelium-dependent dilations along arterioles. Circ Res 2007;101:1292-1299.
15 Alonso F, Boittin FX, Beny JL, Haefliger JA: Loss of connexin40 is associated with decreased endothelium-dependent relaxations and enos levels in the mouse aorta. Am J Physiol Heart Circ Physiol 2010;299:H1365-H1373.
16 de Wit C, Roos F, Bolz SS, Pohl U: Lack of vascular connexin40 is associated with hypertension and irregular arteriolar vasomotion. Physiol Gen 2003;13:169-177.
17 Pfenniger A, Derouette JP, Verma V, Lin X, Foglia B, Coombs W, Roth I, Satta N, Dunoyer-Geindre S, Sorgen P, Taffet S, Kwak BR, Delmar M: Gap junction protein cx37 interacts with endothelial nitric oxide synthase in endothelial cells. Arterioscler Thromb Vasc Biol 2010;30:827-834.
18 Marie I, Beny JL: Calcium imaging of murine thoracic aorta endothelium by confocal microscopy reveals inhomogeneous distribution of endothelial cells responding to vasodilator agents. J Vasc Res 2002;39:260-267.
19 Kirchhoff S, Nelles E, Hagendorff A, Kruger O, Traub O, Willecke K: Reduced cardiac conduction velocity and predisposition to arrhythmias in connexin40-deficient mice. Curr Biol 1998;8:299-302.
20 Boittin FX, Gribi F, Serir K, Beny JL: Ca^{2+}-independent PLA_2 controls endothelial store-operated Ca^{2+} entry and vascular tone in intact aorta. Am J Physiol Heart Circ Physiol 2008;295:H2466-2474.
21 Beny JL, Nguyen MN, Marino M, Matsui M: Muscarinic receptor knockout mice confirm involvement of M3 receptor in endothelium-dependent vasodilatation in mouse arteries. J Cardiovasc Pharmacol 2008;51:505-512.

22 Song P, Sekhon HS, Lu A, Arredondo J, Sauer D, Gravett C, Mark GP, Grando SA, Spindel ER: M3 muscarinic receptor antagonists inhibit small cell lung carcinoma growth and mitogen-activated protein kinase phosphorylation induced by acetylcholine secretion. Cancer Res 2007;67:3936-3944.
23 Zen Y, Fujii T, Yoshikawa S, Takamura H, Tani T, Ohta T, Nakanuma Y: Histological and culture studies with respect to ABCG2 expression support the existence of a cancer cell hierarchy in human hepatocellular carcinoma. Am J Pathol 2007;170:1750-1762.
24 Ryan MJ, Liu B, Herbowy MT, Gross KW, Hajduczok G: Intercellular communication between renin expressing as4.1 cells, endothelial cells and smooth muscle cells. Life Sci 2003;72:1289-1301.
25 Sagar GD, Larson DM: Carbenoxolone inhibits junctional transfer and upregulates connexin43 expression by a protein kinase A-dependent pathway. J Cell Bioch 2006;98:1543-1551.
26 Okamoto T, Akiyama M, Takeda M, Gabazza EC, Hayashi T, Suzuki K: Connexin32 is expressed in vascular endothelial cells and participates in gap-junction intercellular communication. Biochem Biophys Res Commun 2009;382:264-268.
27 Huang TY, Chu TF, Chen HI, Jen CJ: Heterogeneity of $[Ca^{2+}]_i$ signaling in intact rat aortic endothelium. Faseb J 2000;14:797-804.
28 Khurana S, Chacon I, Xie G, Yamada M, Wess J, Raufman JP, Kennedy RH: Vasodilatory effects of cholinergic agonists are greatly diminished in aorta from M3R-/- mice. Eur J Pharmacol 2004;493:127-132.
29 Berra-Romani R, Rinaldi C, Raqeeb A, Castelli L, Magistretti J, Taglietti V, Tanzi F: The duration and amplitude of the plateau phase of ATP- and ADP-evoked Ca^{2+} signals are modulated by ectonucleotidases in in situ endothelial cells of rat aorta. J Vasc Res 2004;41:166-173.
30 Kameritsch P, Pogoda K, Ritter A, Munzing S, Pohl U: Gap junctional communication controls the overall endothelial calcium response to vasoactive agonists. Cardiovasc Res 2012;93:508-515.
31 Christ GJ, Moreno AP, Melman A, Spray DC: Gap junction-mediated intercellular diffusion of Ca^{2+} in cultured human corporal smooth muscle cells. Am J Physiol 1992;263:C373-383.
32 Parthasarathi K, Ichimura H, Monma E, Lindert J, Quadri S, Issekutz A, Bhattacharya J: Connexin 43 mediates spread of Ca^{2+}-dependent proinflammatory responses in lung capillaries. J Clin Invest 2006;116:2193-2200.
33 Saez JC, Connor JA, Spray DC, Bennett MV: Hepatocyte gap junctions are permeable to the second messenger, inositol 1,4,5-trisphosphate, and to calcium ions. Proc Natl Acad Sci USA 1989;86:2708-2712.